Geophysical Research Letters

RESEARCH LETTER
10.1029/2022GL102603

Mesoscale Convective Systems in DYAMOND Global Convection-Permitting Simulations

Zhe Feng[1], L. Ruby Leung[1], Joseph Hardin[1], Christopher R. Terai[2], Fengfei Song[3,4], and Peter Caldwell[2]

[1]Atmospheric Sciences and Global Change Division, Pacific Northwest National Laboratory, Richland, WA, USA, [2]Climate Science Group, Lawrence Livermore National Laboratory, Livermore, CA, USA, [3]Frontier Science Center for Deep Ocean Multispheres and Earth System and Physical Oceanography Laboratory, Ocean University of China, Qingdao, China, [4]Laoshan Laboratory, Qingdao, China

Key Points:

- Deep convective clouds and mesoscale convective systems are tracked in global convection-permitting simulations and satellite observations
- Models produce a diverse range of tropical deep convective systems and MCS frequencies and their proportions in key climate regions
- Models reasonably simulate tropical MCS diurnal cycle and some MCS characteristics, but overestimate MCS precipitation intensity

Supporting Information:

Supporting Information may be found in the online version of this article.

Correspondence to:

Z. Feng,
zhe.feng@pnnl.gov

Citation:

Feng, Z., Leung, L. R., Hardin, J., Terai, C. R., Song, F., & Caldwell, P. (2023). Mesoscale convective systems in DYAMOND global convection-permitting simulations. *Geophysical Research Letters*, *50*, e2022GL102603. https://doi.org/10.1029/2022GL102603

Received 3 JUN 2022
Accepted 22 JAN 2023

Author Contributions:

Conceptualization: Zhe Feng
Data curation: Zhe Feng, Fengfei Song, Peter Caldwell
Formal analysis: Zhe Feng
Funding acquisition: L. Ruby Leung
Investigation: Zhe Feng
Methodology: Zhe Feng
Project Administration: L. Ruby Leung
Software: Zhe Feng, Joseph Hardin, Christopher R. Terai
Supervision: L. Ruby Leung
Validation: Zhe Feng
Visualization: Zhe Feng
Writing – original draft: Zhe Feng

Abstract This study examines the deep convection populations and mesoscale convective systems (MCSs) simulated in the DYAMOND (DYnamics of the atmospheric general circulation modeled on non-hydrostatic domains) winter project. A storm tracking algorithm is applied to six DYAMOND simulations and a global high-resolution satellite cloud and precipitation data set for comparison. The simulated frequencies of tropical deep convection and organized convective systems vary widely among models and regions, although robust MCSs are generally underestimated. The diurnal cycles of MCS initiation and mature stages are well simulated, but the amplitudes are exaggerated over land. Most models capture the observed MCS lifetime, cloud shield area, rainfall volume and movement speed. However, cloud-top height and convective rainfall intensity are consistently overestimated, and stratiform rainfall area and amount are consistently underestimated. Possible causes for the model differences compared to observations and implications for future model developments are discussed.

Plain Language Summary A new class of high-resolution global atmosphere models is emerging for Earth system modeling. These new models can directly simulate convective storm systems and hold promises to improve the simulation of hydrological extremes such as flood-producing rainfall and how they may change in future climate. This study assesses the fidelity of simulated convective storms from six global models against high-resolution satellite observations. We find that the models simulate widely different frequency of convective storms in the tropics, but many do not produce storms that grow as large as observed. Several important aspects of observed storms such as the diurnal cycle, land-ocean contrast, and storm rainfall amount are reasonably captured by the models; however, precipitation intensity is consistently overestimated and the storm rainfall area is too small. We further discussed potential causes for the model differences with observations and future model development needs.

1. Introduction

Organized by mesoscale circulation, cumulonimbus clouds can aggregate into a single storm system with precipitation covering a horizontal scale of 100 km or larger, forming mesoscale convective systems (MCS; Houze, 2004). MCSs produce the majority of precipitation over most of the tropical belt and several regions of the midlatitudes (Feng, Leung, et al., 2021; Nesbitt et al., 2006). With top-heavy latent heating due to the significant amount of stratiform precipitation (Liu et al., 2021; Schumacher & Houze, 2003), MCSs have substantial impacts on the global circulations (Schumacher et al., 2004). Such organized tropical deep convection also dries the surrounding free troposphere, reducing cloud coverage and increasing radiative cooling (Bony et al., 2020). Therefore, organized deep convection is important to the global hydrologic cycle, general circulation, and radiative budget.

Most general circulation models (GCM) with coarse horizontal resolution (~100 km) and parameterized convection (e.g., coupled model intercomparison Project Phase 6, Eyring et al., 2016) cannot simulate MCSs. As MCSs can occupy multiple GCM grid boxes and last much longer than isolated convection (Moncrieff, 2010), many critical processes that maintain MCSs, such as the tight coupling of convective updraft dynamics and cloud microphysics (Fan et al., 2017; Varble et al., 2014a), mesoscale circulations and organized downdrafts associated with stratiform precipitation (Houze et al., 1989; Yang et al., 2017), and vertical momentum transport

Writing – review & editing: Zhe Feng, L. Ruby Leung, Joseph Hardin, Christopher R. Terai, Fengfei Song, Peter Caldwell

(Moncrieff, 1992) are neither resolved nor parameterized. Failure in representing these critical processes has manifested in longstanding biases in simulating many aspects of rainfall variability, such as the distribution of precipitation intensity (Mehran et al., 2014), diurnal cycle (Tang et al., 2021), the Madden-Julian Oscillation (MJO, Hung et al., 2013), among many others (Tian & Dong, 2020).

Convection-permitting models (CPM), with grid-spacings of a few kilometers, allow many convective processes to be explicitly simulated. Regional CPMs can simulate many aspects of MCSs, such as duration, propagation, heavy precipitation, and diurnal cycle (Chen et al., 2021; Feng et al., 2018; Prein, Liu, Ikeda, Bullock, et al., 2017), providing more trustworthy projections of MCS changes in the future (Prein, Liu, Ikeda, Trier, et al., 2017). With increasing computing power, global CPMs can now be used to provide detailed depiction of clouds and convection (Satoh et al., 2019). In the DYAMOND (DYnamics of the Atmospheric general circulation Modeled On Non-hydrostatic Domains) project (Stevens et al., 2019), global CPMs are found to reduce longstanding GCM biases in important aspects of cloud and precipitation such as precipitation diurnal cycle (Stevens et al., 2020), vertical structure of clouds (Roh et al., 2021), and tropical cyclone intensity (Judt et al., 2021).

Several recent studies evaluated various aspects of tropical deep convective clouds and associated anvil cirrus simulated in DYAMOND Phase-I (boreal summer). Christensen and Driver (2021) showed that global CPMs are able to simulate the satellite-observed scaling behavior between convective cloud perimeter and area, although substantial differences among models in the frequency of deep convective cloud size distribution were found. In contrast to traditional GCMs, DYAMOND models generally captured the diurnal cycle of precipitation well both over land and ocean, although the intermodel spread in upper level clouds associated with deep convective updraft detrainment were large (Nugent et al., 2022; Turbeville et al., 2022). Caldwell et al. (2021) showed that the Simple Cloud Resolving E3SM Atmosphere Model (SCREAM) of the Energy Exascale Earth System Model (E3SM) run at 3.25 km grid spacing can capture important weather systems such as tropical and extratropical cyclones, atmospheric rivers and cold air outbreaks, but certain biases in convection and precipitation common to GCMs are not eliminated. It remains unknown how well the DYAMOND models can simulate the global population of deep convective clouds and MCSs.

In this study, we take advantage of the recently developed global MCS tracking methodology and high-resolution satellite observation data sets to examine the realism of the DYAMOND simulations of deep convection populations, with a focus on their associated precipitation and MCS characterstics. Section 2 describes the DYAMOND models and observation data set used, and the MCS tracking methodology; Section 3 presents the analysis results and uncertainties; summary and discussions are provided in Section 4.

2. Data and Methods

2.1. DYAMOND Global Convection-Permitting Models

We evaluate six of the global CPM simulations (see Table S1 in Supporting Information S1) produced for the DYAMOND winter (Phase-II) ensembles (https://www.esiwace.eu/services/dyamond-initiative/services-dyamond-winter). Only a subsample of the DYAMOND models are used because working with the large volume of DYAMOND data is challenging, and the consistency we see across the models we have makes it unlikely that adding more models would affect our major conclusions. Each model simulation was initialized on 20 January 2020 and ran for 40 days till 28 February 2020. The models were initialized with the same European Center for Medium Range Forecasting (ECMWF) Integrated Forecasting Model (IFS). Sea surface temperature are updated at 6-hourly frequency using the IFS output. In this study, only the simulation outputs between February 1 and 28 are used to avoid the model spin up period.

The DYAMOND model simulations were configured with different choices of horizontal and vertical grid spacing and physics parameterization schemes (Stevens et al., 2019). The model horizontal grid spacing examined in this study ranges from 3.0 to 5.0 km (Table S1 in Supporting Information S1). We used hourly model outputs of top-of-atmosphere outgoing longwave radiation (OLR) and surface precipitation to identify and track deep convective systems and MCSs (see Section 2.3).

2.2. Observations

The observational data set used in this study are the NASA Global Merged IR V1 infrared brightness temperature (T_b) data (Janowiak et al., 2017) and the Global Precipitation Measurement (GPM) Integrated Multi-satellitE

Retrievals (IMERG) V06 B precipitation data (Huffman et al., 2019). The global T_b data set combines all geostationary environmental satellites into a near global (60°S–60°N) data set with ∼4 km resolution. The GPM IMERG data set is a unified precipitation retrieval that combines passive microwave sensors and geostationary infrared-based rainfall retrievals. The IMERG data set has a ∼10 km resolution. Both data sets are provided at a native 30 min temporal resolution.

Similar to Feng, Leung, et al. (2021), the global T_b data set is regridded to match the GPM IMERG data set. The 30 min IMERG precipitation data is averaged to hourly, and a snapshot from one of the 30-min T_b data is used to represent convective clouds in an hour. The combined T_b and precipitation data covers 60°S-60°N with a $0.1° \times 0.1°$ and 1-hr resolution. The same period as used by the model simulations (1–28 February 2020) is used for the observations.

2.3. MCS Tracking

To facilitate consistent comparisons between simulated and observed deep convective cloud populations and MCSs, the DYAMOND-simulated OLR and surface precipitation are regridded to conservatively match the coarser $0.1° \times 0.1°$ GPM IMERG grid using the ESMF regridding software (https://earthsystemmodeling.org/regrid/). OLR is converted to T_b following Yang and Slingo (2001).

Deep convective systems (DCSs) are tracked using the open-sourced Python FLEXible object TRacKeR (PyFLEXTRKR) algorithm (Feng et al., 2018, 2022). DCSs are identified and tracked using both T_b and precipitation fields. Briefly, a DCS is defined as contiguous areas with $T_b < 241$ K (cold cloud shield, or CCS) that may contain convective cores ($T_b < 225$ K) and surface precipitation. These T_b were used in Feng, Leung, et al. (2021) to define DCSs. A detect and dilate approach is used to expand the convective cores to encompass the surrounding cold anvil clouds to identify and track DCS. From the tracked DCSs, MCSs are defined as.

1. CCS area $>4 \times 10^4$ km^2 containing a precipitation feature (PF, contiguous area with rain rate >2 mm hr^{-1}) with major axis length >100 km,
2. Various PF characteristics exceed thresholds in Table S2 in Supporting Information S1, and
3. Both criteria 1 and 2 are met continuously for longer than 4 hr.

More details of the MCS tracking algorithm are provided in Feng, Leung, et al. (2021) and the tracking codes are available on GitHub (https://github.com/FlexTRKR/PyFLEXTRKR). Example snapshots of observed and simulated T_b, precipitation, and MCS tracks are provided in Figure S1 in Supporting Information S1.

3. Results

3.1. Deep Convection Population

As the PyFLEXTRKR algorithm tracks all DCSs and identifies MCSs from the tracked DCS population, we can compare both the overall distribution of DCS and those that organize to MCSs.

Over much of the tropics, the DYAMOND models simulate a diverse range of the number of DCSs compared to observations (Figures 1a–1g, 1o), ranging from significantly excessive across the tropics to mostly insufficient globally. For example, the ICON model on average overestimated the number of DCSs by 562% over the Pacific Intertropical Convergence Zone (ITCZ) and to a lesser degree (ranging between 156% and 303%) over other tropical regions. In stark contrast, DCSs are underestimated in the UM model by 16%–62% over all tropical regions. Snapshots of the model simulated convective systems (Figure S1 in Supporting Information S1) over the western Pacific highlight the widely different characteristics of DCSs and precipitation features (e.g., sizes, intensity, and occurrences) associated with both ordinary DCSs and MCSs compared to observations.

Intermodel spread in the simulated number of MCSs is also large although some consistencies emerge (Figures 1h–1n). Most models overestimate both DCSs and MCSs over the Maritime Continent, and four out of six models underestimate tropical MCSs over continents, Indian and Atlantic Ocean and the South Pacific Convergence Zone (SPCZ) (Figure 1p). ICON and SCREAM show similar biases of too frequent DCSs but not enough grow and organize into MCSs. The NICAM model has the relatively smallest differences from observations in this aspect. These conclusions generally hold even when surface precipitation is ignored in defining MCSs (Figure S2 in Supporting Information S1, with the exception of ICON, which has in general far more MCS when surface precipitation is ignored).

10.1029/2022GL102603

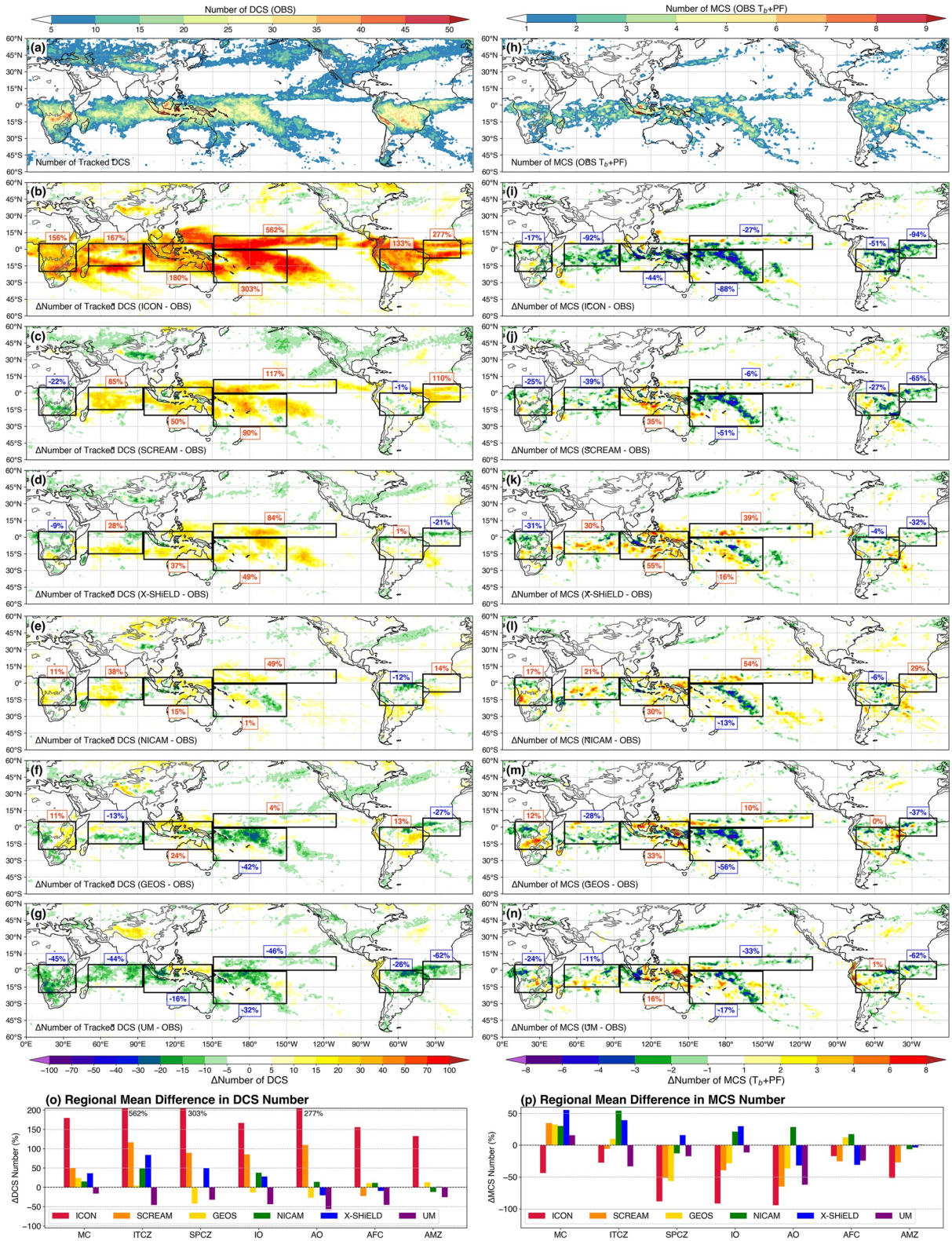

Figure 1. Number of tracked (a)–(g) DCSs and (h–n) MCSs from observations (a),(h) and differences between simulations and observations (b–g, i–n), regional mean differences in percentages of (o) DCSs and (p) MCSs. Black boxes show the boundaries of the regions: MC (Maritime Continent), ITCZ (Intertropical Convergence Zone), SPCZ (South Pacific Convergence Zone), IO (Indian Ocean), AO (Atlantic Ocean), AFC (Africa), and AMZ (Amazon).

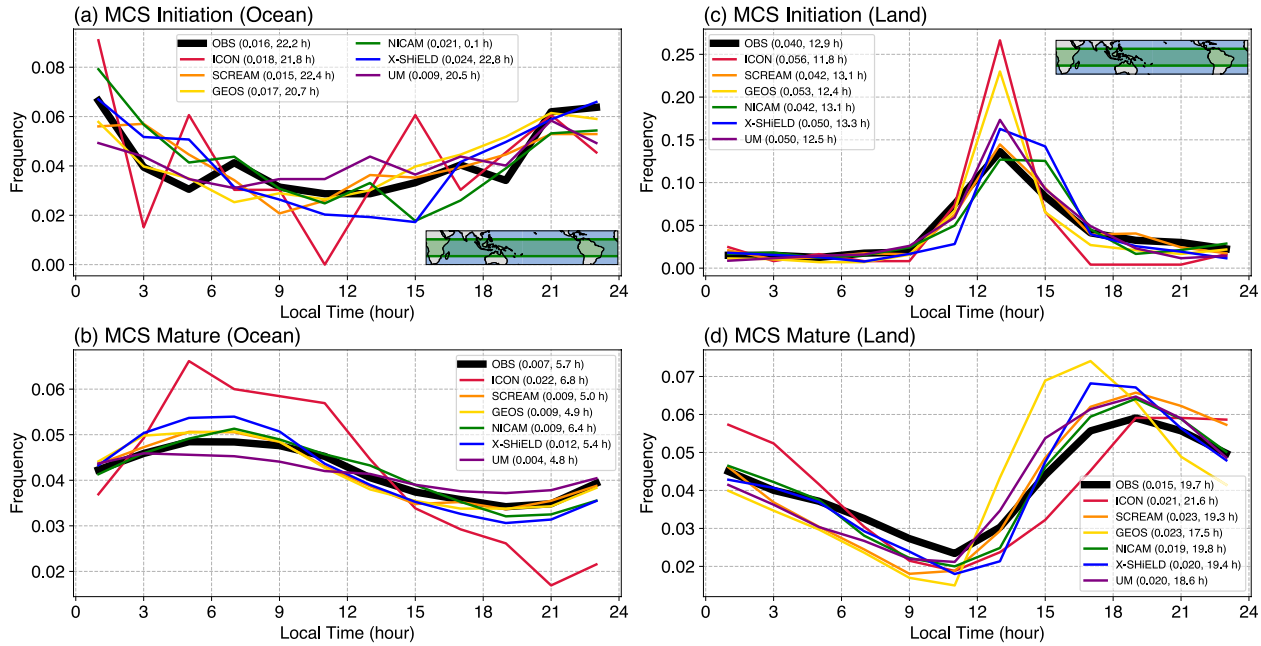

Figure 2. Diurnal cycle of frequencies of tropical MCSs at convection initiation (a),(c) and mature stage (b),(d) over ocean (left column) and land (right column). The amplitude and phase of the diurnal cycles are provided in the legend. Amplitude and phase are calculated using the first harmonic of the Fourier transform applied to the diurnal cycle frequency signal (Wallace, 1975). Area of the tropics included in the anlysis is shown as the green box in the inset (20°S–10°N). An MCS with more than 80% of average PF area fraction over land (ocean) during the first 3 hr of MCS convection initiation is considered a land (ocean) MCS. MCS tracks that start as a split are excluded in this analysis.

We can infer from these results that many DYAMOND models show substantial differences with observations in the proportion of ordinary DCSs and MCSs due to biases in the size and/or persistence of the CCS area. This deficiency has important implications because ordinary DCSs and MCSs have very different vertical profiles of latent heating (Liu et al., 2015), which result in significant differences in the general circulation response that extend beyond the tropics (Schumacher et al., 2004). Precipitation produced by MCSs and ordinary DCSs are further examined in Section 3.4.

3.2. MCS Diurnal Cycle

A key improvement of CPM is a more realistic representation of the diurnal cycle of precipitation (Ban et al., 2021; Stevens et al., 2020). We analyze the diurnal cycle of tropical MCSs to examine the model representation of convection initiation and upscale growth because much of the tropical precipitation is produced by MCSs. We define convection initiation as the first hour a DCS that grows to an MCS is detected, and the MCS mature stage as the hours when the MCS PF major axis length exceeds 100 km.

Convection initiation and MCS mature stage timings are generally well simulated by most models over both land and ocean (Figure 2) as well as the land-ocean contrast in the diurnal cycle amplitudes. In both models and observations, a majority of land MCS initiation occurs during local early afternoon (13–16 LT), and MCSs take several hours to reach the peak mature stage between early evening and midnight (17–24 LT). Oceanic MCSs however, tend to initiate more frequently during the evening hours (20–03 LT), and reach mature stage in the early morning (03–10 LT). The simulated diurnal amplitudes of land MCS mature stage are 27%–54% stronger than observations. This finding is consistent with the stronger simulated total precipitation diurnal cycle found in previous studies (Caldwell et al., 2021; Nugent et al., 2022), suggesting that precipitation from mature MCSs plays an important role in the diurnal cycle difference of total precipitation. The MCS diurnal cycles over different tropical regions are qualitatively consistent with the tropics-wide composites in Figure 2 (not shown), suggesting the models are skillful at capturing the diurnal cycle over different regimes.

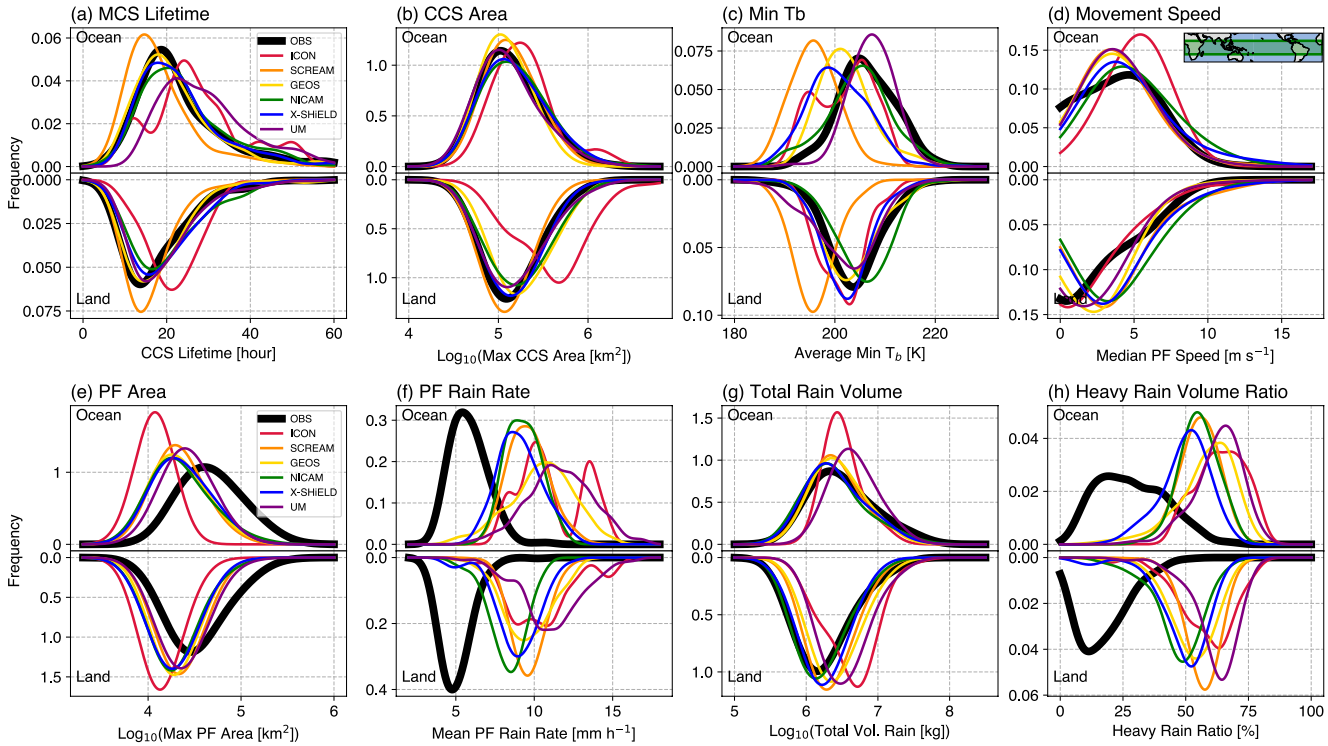

Figure 3. Kernel density estimation of tropical (20°S–10°N) MCS characteristics from observations (thick black line) and simulations (color lines) over ocean (top half in each panel) and over land (bottom half in each panel). (a) MCS lifetime (defined by CCS), (b) maximum CCS area, (c) lifetime-average minimum T_b, (d) median PF movement speed, (e) maximum PF area, (f) mean PF rain rate, (g) lifetime-total rain volume, and (h) heavy rain (rain rate >10 mm hr^{-1}) volume ratio (heavy rain volume/total rain volume). All parameters are calculated over the lifetime and within the CCS mask of each MCS.

3.3. MCS Characteristics

The evolution of individual MCSs is affected by many factors, including their large-scale environments (e.g., water vapor content, convective instability, large-scale vertical motion, vertical wind shear, surface fluxes) and the presence of convection in their vicinity. For simplicity, we focus our analysis on a set of lifetime-representative MCS properties instead of their evolution throughout the MCS lifecycle.

Most DYAMOND models capture the distributions of MCS lifetime, cloud shield area, and lifetime-total rainfall volume (rainfall amount × area) reasonably well, with the exception of the ICON model that produces longer-lived, larger MCSs with more rainfall (Figures 3a, 3b, and 3g). Simulated MCS movement speeds over ocean generally agree with observations, but over land, most models produce slightly faster speeds (Figure 3d), which may indicate stronger cold pools if that is the main mechanism promoting continental MCS movements (Corfidi, 2003; LeMone et al., 1998; Rotunno et al., 1988). Maximum cloud-top heights (proxy by minimum T_b) vary by models, but are generally colder (taller) than observations over ocean, suggesting simulated oceanic convective updraft intensities may be too strong. The most consistent differences with observations are the simulated precipitation characteristics. All models underestimate PF area (i.e., stratiform rain area) while significantly overestimating mean rainfall intensity and heavy rain volume ratio (a proxy for convective rain volume fraction, Figures 3f and 3h).

3.4. Precipitation From MCS and Isolated DCS

In the tropics, most of the precipitation is produced by isolated deep convection and storms with mesoscale structure (Houze et al., 2015). To assess the ability of the DYAMOND models to simulate precipitation from different types of convective storms, we separate the total precipitation into two types of clouds: (1) MCS; (2) isolated deep convection (IDC), defined as non-MCS DCS. This methodology is similar to that used by Chen et al. (2021).

Most DYAMOND models simulate higher frequency of convective precipitation (rain rate >10 mm hr^{-1}) for both MCS and IDC (Figures 4a and 4b). The difference in convective precipitation frequency is larger over

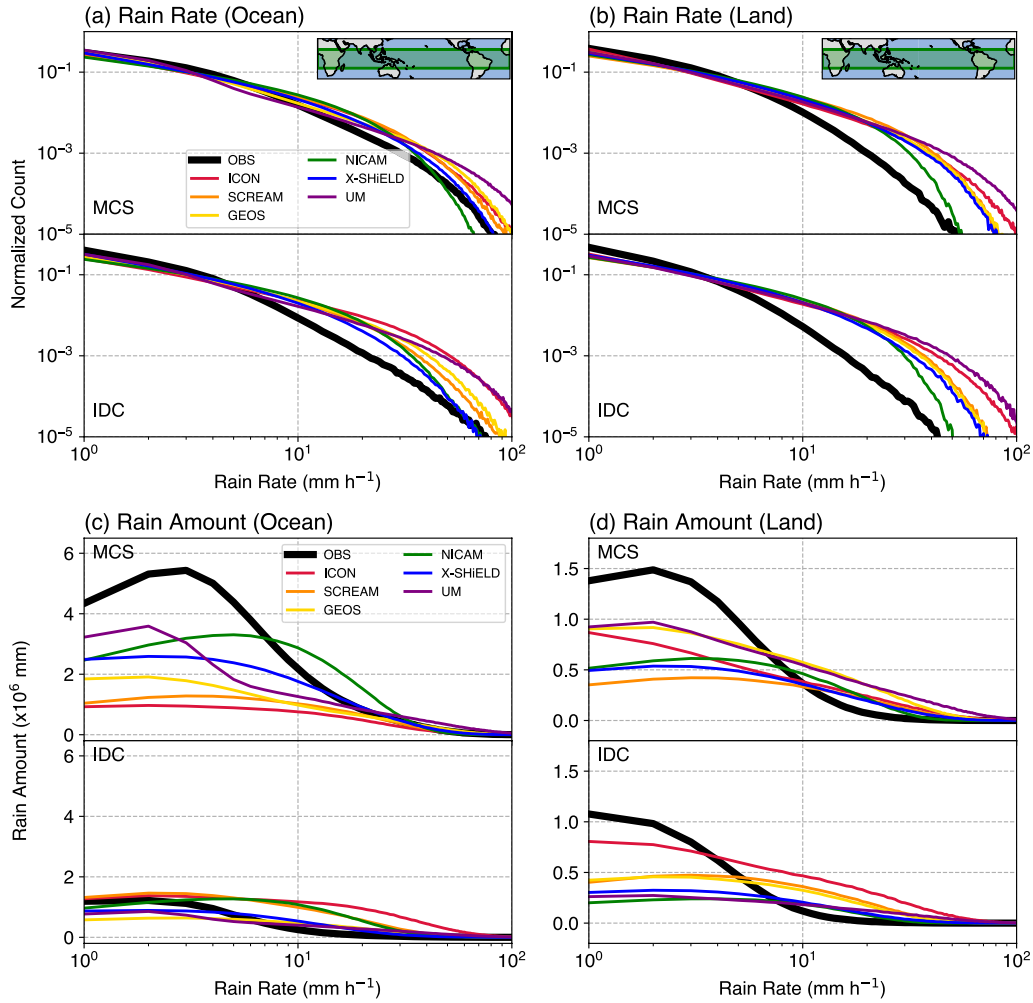

Figure 4. Normalized histogram of hourly rain rates at ~10 km resolution over (a) tropical ocean, (b) tropical land, and rainfall amount by hourly rain rates over (c) tropical ocean and (d) tropical land. Results in (a)–(b) are normalized with respect to the total occurrence in observations and models, respectively; rain amounts in (c)–(d) are calculated by multiplying the counts in (a)–(b) by each rain rate bin center value. Top half in each panel is MCS precipitation and bottom half in each panel is IDC precipitation.

land than over ocean, consistent with the larger mean PF rain rate differences in Figure 3f. The rain amount by rain rate reflects the contribution of absolute precipitation amount from different precipitation intensities. Here, model-simulated MCS stratiform rain (rain rate <10 mm hr^{-1}) amounts are consistently lower than observations over both ocean and land (Figures 4c and 4d), while simulated MCS convective rain amount consistently exceeds the observation over land. On the other hand, the simulated IDCs produce much larger amounts of convective precipitation in most models relative to the observation over land and three out of six models over ocean. These results suggest that the DYAMOND models in general simulate too much intense IDC precipitation, which somewhat counterbalances insufficient MCS precipitation over most of the tropical ocean (Figure S3 in Supporting Information S1).

3.5. Uncertainties in Observations and MCS Tracking

Previous ground-based validation studies found that the IMERG product tends to significantly overestimate the frequency of weak precipitation (<1–2 mm h^{-1}) (Cui et al., 2020; Zhang et al., 2021), suggesting that IMERG tends to exaggerate MCS PF area. Defining MCS PF using areas with rain rate >2 mm hr^{-1} partially alleviates the MCS PF area bias in IMERG over land (see Figure 5 in Feng, Leung, et al., 2021), but PF area over ocean may still be overestimated because stratiform rainfall is more frequent over ocean (Schumacher & Houze, 2003).

On the other hand, IMERG underestimates peak rainfall intensity over land, while convective system rainfall volume is higher (Ayat et al., 2021). These uncertainties in IMERG suggest that the MCS precipitation differences between the models and observations over land (Figures 3 and 4) may be smaller in reality. Nevertheless, the magnitude of the model differences in MCS rainfall area, intensity (Figures 3e and 3f), and stratiform rain amount (Figures 4c and 4d) likely exceed the uncertainties in IMERG.

The MCS definition used in this study is more strict compared to previous studies that use simpler criteria such as only using IR T_b without considering precipitation (Roca et al., 2014) or only using PF area thresholds in satellite snapshots (Liu & Zipser, 2013; Nesbitt et al., 2006). Lowering precipitation criteria and removing the duration-dependence of PF thresholds (Table S3 in Supporting Information S1) do not qualitatively change the differences in the number of MCSs between the DYAMOND simulations and observations (Figure S4 in Supporting Information S1), suggesting the key findings in this study are robust and not particularly sensitive to the MCS definitions.

4. Conclusions

This study examines the deep convection populations and MCSs simulated in DYAMOND Phase-II project. Six DYAMOND model simulations for January–February 2020 are analyzed by applying the PyFLEXTRKR tracking algorithm to both the model outputs and a high-resolution satellite T_b and precipitation data set.

Over much of the tropics, the DYAMOND models simulate a diverse range of the number of DCSs compared to observations, ranging from overestimating by 560% over the Pacific ITCZ to underestimating by 60% over the Atlantic. Intermodel spread in the simulated number of MCSs is also large, although most models overestimate MCSs over the Maritime Continent and underestimate tropical MCSs over the continents, Indian and Atlantic Ocean and the SPCZ (Figure 1). These results indicate that the DYAMOND simulations do not agree on the proportion of ordinary DCSs and MCSs and deviate from observations, which has significant implications because ordinary DCSs and MCSs have very different vertical profiles of latent heating and impact on global circulation. On the other hand, the diurnal timing of MCSs are generally well simulated by most models over both ocean and land, as well as the land-ocean contrast in the diurnal cycle amplitude (Figure 2). However, the simulated diurnal amplitudes of land MCS mature stage are stronger than observations, consistent with the stronger simulated total precipitation diurnal cycle found in previous studies (Caldwell et al., 2021; Nugent et al., 2022).

Most DYAMOND models capture important characteristics of MCSs such as lifetime, cloud shield area and volume rainfall (Figure 3). Simulated MCS movement speeds over ocean generally agree with observations, but over land some models produce faster speeds, which may indicate stronger cold pool intensities that promote MCS movements. Within the simulated MCS cloud shields, models consistently underestimate stratiform rain area and significantly overestimate mean rainfall intensity over both ocean and land, while some models also produce taller cloud-top heights over ocean. DYAMOND models in general simulate higher frequency of grid point level hourly convective precipitation for both MCS and isolated DCS (Figures 4a and 4b), particularly over land. Simulated MCS stratiform rain amounts are consistently lower than observations (Figures 4c and 4d). Most models counterbalance this deficiency by producing excessive isolated DCS precipitation.

These results suggest that the MCS convective intensity in the DYAMOND simulations may be too strong. These differences in simulated MCS properties with observations are consistent with previous studies showing that kilometer-scale regional CPMs produce too wide convective updrafts and too strong updraft velocity, when compared to finer-scale large eddy simulations (Prein et al., 2021; Wang et al., 2020), which leads to stronger convective precipitation efficiency and insufficient stratiform cloud growth. The updraft biases are possibly due to insufficient entrainment-driven dilution of updrafts from turbulent mixing with drier free tropospheric environmental air (Lebo & Morrison, 2015; Morrison et al., 2020). Bulk entrainment rates in the low-to-mid troposphere estimated in CPMs are generally higher over land than over ocean, although it is difficult to identify a simple dependence between entrainment rate and environment (Becker & Hohenegger, 2021). Uncertainties in ice microphysics parameterizations, such as riming, deposition growth, and aggregation may also contribute to the differences with observations (Fan et al., 2017; Han et al., 2019). These deficiencies lead to similar CPM biases in overestimating convective precipitation and underestimating stratiform precipitation in various regimes (Feng et al., 2018; Hagos et al., 2014; Varble et al., 2014b; Zhang et al., 2021).

Despite the deficiencies in simulating certain aspects of observed precipitation characteristics, DYAMOND models with explicit convection show significant improvements in simulating organized convection compared

to GCMs with mesoscale grid spacing (0.25°–0.5°) and parameterized convection. For example, HighResMIP (Haarsma et al., 2016) and comparable models show much weaker MCS precipitation intensity than observations (Feng, Song, et al., 2021; Leung et al., 2022). DYAMOND models also simulate the diurnal cycle of MCSs significantly better, leading to much improved precipitation diurnal cycle over land compared to HighResMIP models (Leung et al., 2022). However, the large intermodel spread in the proportion of ordinary DCSs and MCSs, and the consistent differences in simulated MCS precipitation characteristics (e.g., intensity, size, convective vs. stratiform rain ratio) found in this study suggest that challenges in simulating MCS remain even in current state-of-the-art global CPMs.

Better understanding of the interactions between large-scale environments and simulated tropical convection and precipitation characteristics in global CPMs is needed. An important question is whether the intermodel spread in the DYAMOND model convective population and precipitation characteristics is caused by differences in the simulated large-scale environments and associated circulation-convection feedback or by the differences in model treatments of physics parameterizations such as turbulence and microphysics. Global CPM simulations are computationally expensive, limiting efforts in model tuning and evaluation of parametric uncertainty. More process-oriented and phenomena-based model diagnostics (Leung et al., 2022), such as those performed in this study, can provide important guidance for model tuning and further model development as well as improve our understanding of convection-environment interactions.

Data Availability Statement

Model and observation data analyzed and analysis and visualization codes in this study can be accessed at https://doi.org/10.5281/zenodo.7633894. The PyFLEXTRKR tracking codes are available on GitHub (https://github.com/FlexTRKR/PyFLEXTRKR).

Acknowledgments

This study is supported by the US Department of Energy Office of Science Biological and Environmental Research (BER) as part of the Regional and Global Climate Modeling program through the Water Cycle and Climate Extremes Modeling (WACCEM) scientific focus area. Data analyses described in this study were performed using computational resources provided by the National Energy Research Scientific Computing Center (NERSC), a DOE Office of Science User Facility supported by the Office of Science of the US Department of Energy under contract DEAC02-05CH11231. DYAMOND data management was provided by the German Climate Computing Center (DKRZ) and supported through the projects ESiWACE and ESiWACE2. The projects ESiWACE and ESiWACE2 have received funding from the European Union's Horizon 2020 research and innovation programme under Grants 675191 and 823988. This work used resources of the Deutsches Klimarechenzentrum (DKRZ) granted by its Scientific Steering Committee (WLA) under project IDs bk1040 and bb1153. PNNL is operated for DOE by Battelle Memorial Institute under contract DE-AC05-76RL01830. The work of CRT and PC was supported as part of the Energy Exascale Earth System Model (E3SM) project and was performed under the auspices of the DOE by Lawrence Livermore National Laboratory under Contract DE-AC52-07NA27344.

References

Ayat, H., Evans, J. P., Sherwood, S., & Behrangi, A. (2021). Are storm characteristics the same when viewed using merged surface radars or a merged satellite product? *Journal of Hydrometeorology*, *22*(1), 43–62. https://doi.org/10.1175/jhm-d-20-0187.1

Ban, N., Caillaud, C., Coppola, E., Pichelli, E., Sobolowski, S., Adinolfi, M., et al. (2021). The first multi-model ensemble of regional climate simulations at kilometer-scale resolution, part I: Evaluation of precipitation. *Climate Dynamics*, *57*(1–2), 275–302. https://doi.org/10.1007/s00382-021-05708-w

Becker, T., & Hohenegger, C. (2021). Entrainment and its dependency on environmental conditions and convective organization in convection-permitting simulations. *Monthly Weather Review*, *149*(2), 537–550. https://doi.org/10.1175/MWR-D-20-0229.1

Bony, S., Semie, A., Kramer, R. J., Soden, B., Tompkins, A. M., & Emanuel, K. A. (2020). Observed modulation of the tropical radiation budget by deep convective organization and lower-tropospheric stability. *AGU Advances*, *1*(3), e2019AV000155. https://doi.org/10.1029/2019AV000155

Caldwell, P. M., Terai, C. R., Hillman, B., Keen, N. D., Bogenschutz, P., Lin, W., et al. (2021). Convection-permitting simulations with the E3SM global atmosphere model. *Journal of Advances in Modeling Earth Systems*, *13*(11), e2021MS002544. https://doi.org/10.1029/2021MS002544

Chen, X., Leung, L. R., Feng, Z., & Song, F. (2021). Crucial role of mesoscale convective systems in the vertical mass, water and Energy transports of the South Asian summer monsoon. *Journal of Climate*, 1–46. https://doi.org/10.1175/JCLI-D-21-0124.1

Christensen, H. M., & Driver, O. G. A. (2021). The fractal nature of clouds in global storm-resolving models. *Geophysical Research Letters*, *48*(23), e2021GL095746. https://doi.org/10.1029/2021GL095746

Corfidi, S. F. (2003). Cold pools and MCS propagation: Forecasting the motion of downwind-developing MCSs. *Weather and Forecasting*, *18*(6), 997–1017. https://doi.org/10.1175/1520-0434(2003)018<0997:CPAMPF>2.0.CO;2

Cui, W., Dong, X., Xi, B., Feng, Z., & Fan, J. (2020). Can the GPM IMERG final product accurately represent MCSs' precipitation characteristics over the Central and Eastern United States? *Journal of Hydrometeorology*, *21*(1), 39–57. https://doi.org/10.1175/JHM-D-19-0123.1

Eyring, V., Bony, S., Meehl, G. A., Senior, C. A., Stevens, B., Stouffer, R. J., & Taylor, K. E. (2016). Overview of the coupled model intercomparison project phase 6 (CMIP6) experimental design and organization. *Geoscientific Model Development*, *9*(5), 1937–1958. https://doi.org/10.5194/gmd-9-1937-2016

Fan, J., Han, B., Varble, A., Morrison, H., North, K., Kollias, P., et al. (2017). Cloud-resolving model intercomparison of an MC3E squall line case: Part I—Convective updrafts. *Journal of Geophysical Research: Atmospheres*, *122*(17), 9351–9378. https://doi.org/10.1002/2017JD026622

Feng, Z., Hardin, J., Barnes, H. C., Leung, L. R., Varble, A., & Zhang, Z. (2022). PyFLEXTRKR: A flexible feature tracking Python software for convective cloud analysis [Dataset]. EGUsphere [preprint]. https://doi.org/10.5194/egusphere-2022-1136

Feng, Z., Leung, L. R., Houze, R. A., Hagos, S., Hardin, J., Yang, Q., et al. (2018). Structure and evolution of mesoscale convective systems: Sensitivity to cloud microphysics in convection-permitting simulations over the United States. *Journal of Advances in Modeling Earth Systems*, *10*(7), 1470–1494. https://doi.org/10.1029/2018MS001305

Feng, Z., Leung, L. R., Liu, N., Wang, J., Houze, R. A., Li, J., et al. (2021). A global high-resolution mesoscale convective system database using satellite-derived cloud tops, surface precipitation, and tracking. *Journal of Geophysical Research: Atmospheres*, *126*(8). https://doi.org/10.1029/2020JD034202

Feng, Z., Song, F., Sakaguchi, K., & Leung, L. R. (2021). Evaluation of mesoscale convective systems in climate simulations: Methodological development and results from MPAS-CAM over the United States. *Journal of Climate*, *34*(7), 2611–2633. https://doi.org/10.1175/JCLI-D-20-0136.1

Haarsma, R. J., Roberts, M. J., Vidale, P. L., Senior, C. A., Bellucci, A., Bao, Q., et al. (2016). High resolution model intercomparison project (HighResMIP v1.0) for CMIP6. *Geoscientific Model Development*, *9*(11), 4185–4208. https://doi.org/10.5194/gmd-9-4185-2016

Hagos, S., Feng, Z., Burleyson, C. D., Lim, K. S. S., Long, C. N., Wu, D., & Thompson, G. (2014). Evaluation of convection-permitting model simulations of cloud populations associated with the Madden-Julian Oscillation using data collected during the AMIE/DYNAMO field campaign. *Journal of Geophysical Research-Atmospheres*, *119*(21), 12052–12068. https://doi.org/10.1002/2014JD022143

Han, B., Fan, J., Varble, A., Morrison, H., Williams, C. R., Chen, B., et al. (2019). Cloud-Resolving model intercomparison of an MC3E squall line case: Part II. Stratiform precipitation properties. *Journal of Geophysical Research: Atmospheres*, *124*(2), 1090–1117. https://doi.org/10.1029/2018JD029596

Houze, R. A. (2004). Mesoscale convective systems. *Reviews of Geophysics*, *42*(4), RG4003. https://doi.org/10.1029/2004RG000150

Houze, R. A., Jr., Rasmussen, K. L., Zuluaga, M. D., & Brodzik, S. R. (2015). The variable nature of convection in the tropics and subtropics: A legacy of 16 years of the tropical rainfall measuring mission satellite. *Reviews of Geophysics*, *53*(3), 994–1021. https://doi.org/10.1002/2015rg000488

Houze, R. A., Rutledge, S. A., Biggerstaff, M. I., & Smull, B. F. (1989). Interpretation of Doppler weather radar displays of midlatitude mesoscale convective systems. *Bulletin of the American Meteorological Society*, *70*(6), 608–619. https://doi.org/10.1175/1520-0477(1989)070<0608:iodwrd>2.0.co;2

Huffman, G. J., Stocker, E. F., Bolvin, D. T., Nelkin, E. J., & Tan, J. (2019). GPM IMERG final precipitation L3 half hourly 0.1 degree x 0.1 degree V06. https://doi.org/10.5067/GPM/IMERG/3B-HH/06

Hung, M.-P., Lin, J.-L., Wang, W., Kim, D., Shinoda, T., & Weaver, S. J. (2013). MJO and convectively coupled equatorial waves simulated by CMIP5 climate models. *Journal of Climate*, *26*(17), 6185–6214. https://doi.org/10.1175/JCLI-D-12-00541.1

Janowiak, J., Joyce, B., & Xie, P. (2017). NCEP/CPC L3 half hourly 4km global (60S - 60N) Merged IR V1. https://doi.org/10.5067/P4HZB9N27EKU

Judt, F., Klocke, D., Rios-Berrios, R., Vanniere, B., Ziemen, F., Auger, L., et al. (2021). Tropical cyclones in global storm-resolving models. *Journal of the Meteorological Society of Japan. Ser. II*, *99*(3), 579–602. https://doi.org/10.2151/jmsj.2021-029

Lebo, Z. J., & Morrison, H. (2015). Effects of horizontal and vertical grid spacing on mixing in simulated squall lines and implications for convective Strength and structure. *Monthly Weather Review*, *143*(11), 4355–4375. https://doi.org/10.1175/MWR-D-15-0154.1

LeMone, M. A., Zipser, E. J., & Trier, S. B. (1998). The role of environmental shear and thermodynamic conditions in determining the structure and evolution of mesoscale convective systems during TOGA COARE. *Journal of the Atmospheric Sciences*, *55*(23), 3493–3518. https://doi.org/10.1175/1520-0469(1998)055<3493:TROESA>2.0.CO;2

Leung, L. R., Boos, W. R., Catto, J. L., DeMott, C., Martin, G. M., Neelin, J. D., et al. (2022). Exploratory precipitation metrics: Spatiotemporal characteristics, process-oriented, and phenomena-based. *Journal of Climate*, *35*(12), 1–55. https://doi.org/10.1175/JCLI-D-21-0590.1

Liu, C., Shige, S., Takayabu, Y. N., & Zipser, E. (2015). Latent heating contribution from precipitation systems with different sizes, depths, and intensities in the tropics. *Journal of Climate*, *28*(1), 186–203. https://doi.org/10.1175/JCLI-D-14-00370.1

Liu, C. T., & Zipser, E. (2013). Regional variation of morphology of organized convection in the tropics and subtropics. *Journal of Geophysical Research-Atmospheres*, *118*(2), 453–466. https://doi.org/10.1029/2012JD018409

Liu, N., Leung, L. R., & Feng, Z. (2021). Global mesoscale convective system latent heating characteristics from GPM retrievals and an MCS tracking dataset. *Journal of Climate*, *34*(21), 8599–8613. https://doi.org/10.1175/JCLI-D-20-0997.1

Mehran, A., AghaKouchak, A., & Phillips, T. J. (2014). Evaluation of CMIP5 continental precipitation simulations relative to satellite-based gauge-adjusted observations. *Journal of Geophysical Research: Atmospheres*, *119*(4), 1695–1707. https://doi.org/10.1002/2013JD021152

Moncrieff, M. W. (1992). Organized convective systems: Archetypal dynamical models, mass and momentum flux theory, and parametrization. *Quarterly Journal of the Royal Meteorological Society*, *118*(507), 819–850. https://doi.org/10.1002/qj.49711850703

Moncrieff, M. W. (2010). The multiscale organization of moist convection and the Intersection of weather and climate. In *Climate Dynamics: Why Does Climate Vary? Geophysical Monograph Series* (Vol. 189, pp. 3–26). American Geophysical Union.

Morrison, H., Peters, J. M., Varble, A. C., Hannah, W. M., & Giangrande, S. E. (2020). Thermal chains and entrainment in cumulus updrafts. Part I: Theoretical description. *Journal of the Atmospheric Sciences*, *77*(11), 3637–3660. https://doi.org/10.1175/JAS-D-19-0243.1

Nesbitt, S. W., Cifelli, R., & Rutledge, S. A. (2006). Storm morphology and rainfall characteristics of TRMM precipitation features. *Monthly Weather Review*, *134*(10), 2702–2721. https://doi.org/10.1175/mwr3200.1

Nugent, J. M., Turbeville, S. M., Bretherton, C. S., Blossey, P. N., & Ackerman, T. P. (2022). Tropical cirrus in global storm-resolving models: 1. Role of deep convection. *Earth and Space Science*, *9*(2), e2021EA001965. https://doi.org/10.1029/2021EA001965

Prein, A., Liu, C., Ikeda, K., Bullock, R., Rasmussen, R., Holland, G., & Clark, M. (2017). Simulating North American mesoscale convective systems with a convection-permitting climate model. *Climate Dynamics*, *55*(1–2), 95–110. https://doi.org/10.1007/s00382-017-3993-2

Prein, A. F., Liu, C. H., Ikeda, K., Trier, S. B., Rasmussen, R. M., Holland, G. J., & Clark, M. P. (2017). Increased rainfall volume from future convective storms in the US. *Nature Climate Change*, *7*(12), 880–884. https://doi.org/10.1038/s41558-017-0007-7

Prein, A. F., Rasmussen, R. M., Wang, D., & Giangrande, S. E. (2021). Sensitivity of organized convective storms to model grid spacing in current and future climates. *Philosophical Transactions of the Royal Society A: Mathematical, Physical & Engineering Sciences*, *379*(2195), 20190546. https://doi.org/10.1098/rsta.2019.0546

Roca, R., Aublanc, J., Chambon, P., Fiolleau, T., & Viltard, N. (2014). Robust observational quantification of the contribution of mesoscale convective systems to rainfall in the tropics. *Journal of Climate*, *27*(13), 4952–4958. https://doi.org/10.1175/JCLI-D-13-00628.1

Roh, W., Satoh, M., & Hohenegger, C. (2021). Intercomparison of cloud properties in DYAMOND simulations over the Atlantic Ocean. *Journal of the Meteorological Society of Japan. Ser. II*, *99*(6), 1439–1451. https://doi.org/10.2151/jmsj.2021-070

Rotunno, R., Klemp, J. B., & Weisman, M. L. (1988). A theory for strong, Long-lived squall lines. *Journal of the Atmospheric Sciences*, *45*(3), 463–485. https://doi.org/10.1175/1520-0469(1988)045<0463:ATFSLL>2.0.CO;2

Satoh, M., Stevens, B., Judt, F., Khairoutdinov, M., Lin, S.-J., Putman, W. M., & Düben, P. (2019). Global cloud-resolving models. *Current Climate Change Reports*, *5*(3), 172–184. https://doi.org/10.1007/s40641-019-00131-0

Schumacher, C., & Houze, R. A. (2003). Stratiform rain in the tropics as seen by the TRMM precipitation radar. *Journal of Climate*, *16*(11), 1739–1756. https://doi.org/10.1175/1520-0442(2003)016<1739:SRITTA>2.0.CO;2

Schumacher, C., Houze, R. A., & Kraucunas, I. (2004). The tropical dynamical response to latent heating estimates derived from the TRMM precipitation radar. *Journal of the Atmospheric Sciences*, *61*(12), 1341–1358. https://doi.org/10.1175/1520-0469(2004)061<1341:TTDRTL>2.0.CO;2

Stevens, B., Acquistapace, C., Hansen, A., Heinze, R., Klinger, C., Klocke, D., et al. (2020). The added value of large-eddy and storm-resolving models for simulating clouds and precipitation. *Journal of the Meteorological Society of Japan. Ser. II*, *98*(2), 395–435. https://doi.org/10.2151/jmsj.2020-021

Stevens, B., Satoh, M., Auger, L., Biercamp, J., Bretherton, C. S., Chen, X., et al. (2019). Dyamond: The DYnamics of the atmospheric general circulation modeled on non-hydrostatic Domains. *Progress in Earth and Planetary Science*, *6*(1), 61. https://doi.org/10.1186/s40645-019-0304-z

Tang, S., Gleckler, P., Xie, S., Lee, J., Ahn, M.-S., Covey, C., & Zhang, C. (2021). Evaluating diurnal and semi-diurnal cycle of precipitation in CMIP6 models using satellite- and ground-based observations. *Journal of Climate*, 1–56. https://doi.org/10.1175/jcli-d-20-0639.1

Tian, B., & Dong, X. (2020). The double-ITCZ bias in CMIP3, CMIP5, and CMIP6 models based on annual mean precipitation. *Geophysical Research Letters*, *47*(8), e2020GL087232. https://doi.org/10.1029/2020GL087232

Turbeville, S. M., Nugent, J. M., Ackerman, T. P., Bretherton, C. S., & Blossey, P. N. (2022). Tropical cirrus in global storm-resolving models: 2. Cirrus life cycle and top-of-atmosphere radiative fluxes. *Earth and Space Science*, *9*(2), e2021EA001978. https://doi.org/10.1029/2021EA001978

Varble, A., Zipser, E. J., Fridlind, A. M., Zhu, P., Ackerman, A. S., Chaboureau, J.-P., et al. (2014a). Evaluation of cloud-resolving and limited area model intercomparison simulations using TWP-ICE observations: 1. Deep convective updraft properties. *Journal of Geophysical Research: Atmospheres*, *119*(24), 13–918. https://doi.org/10.1002/2013JD021371

Varble, A., Zipser, E. J., Fridlind, A. M., Zhu, P., Ackerman, A. S., Chaboureau, J.-P., et al. (2014b). Evaluation of cloud-resolving and limited area model intercomparison simulations using TWP-ICE observations: 2. Precipitation microphysics. *Journal of Geophysical Research: Atmospheres*, *119*(24), 2013JD021372. https://doi.org/10.1002/2013JD021372

Wallace, J. M. (1975). Diurnal Variations in precipitation and Thunderstorm frequency over the Conterminous United States. *Monthly Weather Review*, *103*(5), 406–419. Retrieved from https://journals.ametsoc.org/doi/abs/10.1175/1520-0493%281975%29103%3C0406%3ADVIPAT%3E2.0.CO%3B2

Wang, D., Giangrande, S. E., Feng, Z., Hardin, J. C., & Prein, A. F. (2020). Updraft and downdraft core size and intensity as revealed by radar wind profilers: MCS observations and idealized model comparisons. *Journal of Geophysical Research: Atmospheres*, *125*(11), e2019JD031774. https://doi.org/10.1029/2019JD031774

Yang, Q., Houze, R. A., Leung, L. R., & Feng, Z. (2017). Environments of long-lived mesoscale convective systems over the Central United States in convection permitting climate simulations. *Journal of Geophysical Research: Atmospheres*, *122*(24), 13288–13307. https://doi.org/10.1002/2017JD027033

Yang, G. Y., & Slingo, J. (2001). The diurnal cycle in the Tropics. *Monthly Weather Review*, *129*(4), 784–801. https://doi.org/10.1175/1520-0493(2001)129%3C0784:TDCITT%3E2.0.CO;2

Zhang, Z., Varble, A., Feng, Z., Hardin, J., & Zipser, E. (2021). Growth of mesoscale convective systems in observations and a seasonal convection-permitting simulation over Argentina. *Monthly Weather Review*, *149*(10), 3469–3490. https://doi.org/10.1175/MWR-D-20-0411.1